This is an open-access article under the CC BY-NC-ND license (http://creativecommons.org/licenses/by-nc-nd/4.0/)

P-ISSN: 2304-3075; E-ISSN: 2305-4360
International Journal of Veterinary Science
www.ijvets.com; editor@ijvets.com

Research Article https://doi.org/10.47278/journal.ijvs/2025.050

Green Synthesis of Silver Nanoparticles by Thymus Vulgaris; Synthesis, Characterization and Application in Healing of Metacarpal and Metatarsal Bone Fractures in Sheep and Goats

Madeh Sadan [1,*], Ahmed A. H. Abdellatif [2], Mohie Haridy [3], Abdulla Al-Hawas[4] and Walid Refaai [4]

[1]Department of Clinical Sciences, College of Veterinary Medicine, Qassim University, P.O. Box 6622, Buraidah, 51452, Saudi Arabia
[2]Department of Pharmaceutics, College of Pharmacy, Qassim University, P.O. Box 6622, Buraidah, 51452, Saudi Arabia
[3]Department of Pathology and Laboratory Diagnosis, College of Veterinary Medicine, Qassim University, P.O. Box 6622, Buraidah, 51452, Saudi Arabia
[4]Department of Surgery, Anesthesiology and Radiology, University Veterinary Hospital, Qassim University, P.O. Box 6622, Buraidah, 51452, Saudi Arabia
***Corresponding author:** m.sadan@qu.edu.sa

Article History: 25-083 Received: 20-Mar-25 Revised: 17-Apr-25 Accepted: 18-Apr-25 Online First: 06-May-25

ABSTRACT

Long bones injuries and fractures are common orthopedic problems occur in sheep and goats. This study aimed to evaluate fractures of the metacarpal and metatarsal bones in sheep and goats (clinical study) and to describe the accelerating action of silver nanoparticles *Thymus vulgaris* (Ag-NPs-THV) on healing process of fracture in goats (experimental study). AgNPs were reduced using THV to form AgNPs-THV. The formulated AgNPs-THV was characterized for size, charge, morphology, and the drug content of THV was determined for further experiments. Twenty-four adult male Barbary goats were randomly assigned into two equal groups. A cortical bone defect 3.5mm diameter was made at the middle third of the right metacarpal bone in each goat. Group 1 (THV Extract) and Group 2 (AgNPs-THV) were injected with THV extract liquid, and AgNPs-THV at the bone defect, respectively. The healing process was evaluated for eight weeks after surgery depending on the radiological, turnover biomarkers of bone, and histopathological assessment. Additionally, 49 sheep and goats with metacarpal and metatarsal bone fractures were included in this study on the basis of clinical, and radiographical examinations. The formulated AgNPs-THV was oval and formed as cluster. The size was in nano range, while the charge was -18.1±1.74mV. Furthermore, the recorded wavelength was 388.5±2.2nm, and THV was recorded in AgNPs-THV as 5765.336µg/mL. The radiographic union scale was significantly affected by treatment and time, $P<0.001$. AgNPs-THV significantly provided better radiographic union scale than that provided by THV Extract at 2,5 and 8 weeks post treatment. Histopathologically, at 5 weeks post-operative, Ag-NPs-THV treated group showed a significant decrease of fracture gap that filled with woven bone beside lamellar bone in comparison with THV Extract group ($P<0.01$) that still had wider gap filled with granulation tissue and limited woven bone. At 8 weeks post-treatment, 100% of cases treated with Ag-NPs-THV showed complete healing with lamellar bone compared with 50% of THV extract treated group. Ag-NPs-THV colloidal nano-formulation could be used as a promising formulation to speed up healing process of tibial bone fracture in rabbit.

Key words: Diagnostic imaging; Pathology; Pathophysiology; Ruminant; *Thymus vulgaris.*

INTRODUCTION

Fractures and injuries of bones are major affections because they lead to economic and health losses of animals. Veterinary researchers try to initiate the progress of the healing process of fracture and bone injuries. Car accidents, falls and crush injuries are the main causes of fractures (Farooq et al. 2023). Fractures and bone injuries can significantly affect animal's health and quality of life. Various complications such as healing disorders including;

Cite This Article as: Sadan M, Abdellatif AAH, Haridy M, Al-Hawas A and Refaai W, 2025. Green synthesis of silver nanoparticles by *Thymus vulgaris*; synthesis, characterization, and application in healing of metacarpal and metatarsal bone fractures in sheep and goats. International Journal of Veterinary Science x(x): xxxx. https://doi.org/10.47278/journal.ijvs/2025.050

union deformities are important challenges that face orthopedic surgeons and researchers when handling fractures. As a result, researchers are currently search for the ideal techniques to overcome long-term side effects and complications of fractures and bone injuries (Jahangirbasha et al. 2019).

Healing process of bone consisted of three overlapping phases named; the inflammatory, reparative, and remodeling. the inflammatory phase is very important phase in the healing process, which is affected by both the local and systemic factors related to the cause of injuries and fractures (Sravanti et al. 2022; Sindhu et al. 2024). Green synthesis nanoparticles are increasingly used to overcome various disorders in human and animal practice (Abdellatif et al. 2022a; Abdellatif et al. 2022b; Abdellatif et al. 2022c). Plant-based medicine including herbal extracts is widely trusted and used by over 75% of people globally for primary healthcare, treatment of various disorders (Vijayaram et al. 2024; Abdellatif et al. 2024; Sadan et al. 2024; Sadan et al. 2025). Silver NPs (AgNPs) have a pronounced antibacterial effect (Abdellatif et al. 2021a) and are used in different applications, including drug delivery, coating of devices (Abdelhamed et al. 2022; Selmi et al. 2022) and regenerative materials (Ansar et al. 2020). It was established that AgNPs had shown a promising active role in wound healing. AgNPs can also promote wound contraction and stimulate proliferation of keratinocytes (Vimalraj 2020).

Silver nanoparticles (AgNPs) have the potential to overcome the constraints associated with traditional nanoparticles (NPs) by employing passive targeting methods after the disease has been identified. In addition to being an antioxidant, anti-inflammatory, pain-relieving, antibacterial, anti-inflammatory and anticancer agent, *Thymus vulgaris* (Thymol) is a phytonutrient, which is a naturally occurring substance that may be found in plants (Abdelhamed et al. 2022). In recent years, there has been a growing interest in using silver nanoparticles for medical applications due to their unique properties such as high surface area, biocompatibility, and antimicrobial activity. These properties make them an ideal candidate for use in surgical repair of fractures (Xu et al. 2020).

One area where AgNPs synthesized using *Thymus vulgaris* could have a significant impact is in the development of synthetic bone scaffolds (Abdellatif et al. 2023). Bone scaffolds are used in medical procedures to support the growth of new bone tissue. However, traditional scaffolds can be prone to infection, which can lead to complications and slow down the healing process. Antibacterial AgNPs can be used to dope synthetic bone scaffolds to avoid infections. The antibacterial activity of AgNPs-implanted crystalline hydroxyapatite (HA) or titanium scaffolds is strong against Gram-positive and Gram-negative microorganisms. This could potentially reduce the risk of infection and improve the success rate of bone scaffolding procedures (Marsich et al. 2013; Qing et al. 2018).

Green synthesis using *Thymus vulgaris* to create AgNPs has several advantages over traditional synthesis methods (Abdellatif et al. 2022a). For one, it is eco-friendlier and reduces the use of toxic chemicals. It is also cost-effective, as *Thymus vulgaris* is a readily available and affordable herb (Abdellatif et al. 2022b; Abdellatif et al. 2022c). Additionally, green synthesis using *Thymus vulgaris* extract can produce AgNPs with a narrower size distribution compared to traditional synthesis methods, which can improve their effectiveness in various applications (Abdellatif et al. 2022b; Abdellatif et al. 2023). A recent experiment has shown promising results in the use of silver nanoparticles synthesized with Thymus vulgaris against *Candida albicans*, the antifungal activity (Mohammadi et al. 2019) for future surgical repair of metacarpal and metatarsal fractures. The use of Thymus vulgaris in the synthesis of silver nanoparticles is particularly interesting as it is a natural and environmentally friendly method of production (Azadi et al. 2021). In addition to its environmental benefits, the use of Thymus vulgaris in the synthesis of silver nanoparticles also has potential health benefits. Thymus vulgaris has long been used in traditional medicine for its anti-inflammatory and antimicrobial properties and its incorporation into silver nanoparticle synthesis could enhance these properties (Aldosary et al. 2021).

In general, the use of silver nanoparticles synthesized with *Thymus vulgaris* for surgical repair of fractures is an exciting development in the field of medical research. Its unique properties provide a safe and effective alternative to traditional methods of surgical repair, while its natural and environmentally friendly method of production makes it a potential game-changer in the world of medicine. If further studies can confirm these results, it could revolutionize the way we approach surgical repair of fractures and pave the way for a safer and more sustainable future. In spite of fracture's popularity, little was found in the literature about effect of Ag-NPs-THV on the healing of fracture, therefore is the first research evaluating the use of AgNPs- THV in acceleration of the healing of metacarpal and metatarsal bone fractures in sheep and goats. Therefore, this study was designed to evaluate metacarpal and metatarsal bones fractures in sheep and goats and to describe the accelerating action of AgNPs-THV on fracture bone healing in goats.

MATERIALS AND METHODS

Ethical approval of the study

The study protocol was approved by the Animal Welfare and Ethics Committee of Qassim University. The protocol of the research was approved (No. 367) by the Committee for Animal Welfare and Ethics in accordance with the Laboratory Animal Control Guidelines of Qassim University.

Preparation of AgNPs-THV

The colloidal AgNPs-THV were synthesized eco-friendly as the previously prepared method (Varghese et al. 2019). The THV seeds were soaked for 6h for extraction. Then the seeds of THVs were boiled in 100mL distilled water for 20min to extract the THV's active constituents. The supernatant was collected and stored in a brown bottle for next step. The extract of THV was mixed with fresh solution of 1mM AgNO3 and incubated with stirring at 1000rpm overnight. The formulated AgNPs-THV were changed to deep brown color upon addition of AgNO3 to the extract of THV. The obtained AgNPs-THV was purified with centrifugation and stored for dark place for next experiment.

Size and ζ-potential of AgNPs-THV

The samples of AgNPs-THV were sonicated for 15min using water bath sonicator and vortexed for 2min then diluted 1:4 with deionized water before measurement. The particle size and size distribution in terms of average volume diameters and polydispersity index were analyzed by photon correlation spectroscopy using particle size analyzer Dynamic Light Scattering (DLS) (Zetasizer Nano ZN, Malvern Panalytical Ltd, UK) at fixed angle 173° at 25° C. Three samples were tested. The same device measured zeta potential (Abdellatif and Tawfeek 2016; Abdellatif et al. 2018; Abdellatif et al. 2020; Abdellatif et al. 2021a; Abdellatif et al. 2021b).

UV-VIS spectroscopy of AgNPs-THV

The absorbance spectra of AgNPs-THV was also determined and measured using a UV-VIS absorbance spectrophotometer (Lambda 25, Perkin Elmer, Singapore) (Abdellatif et al. 2020; Abdellatif et al. 2021a; Abdellatif et al. 2021b).

Morphology of AgNPs-THV

The shape and morphology of AgNPs-THV was imaged and captured scanning electron microscope (SEM) made by JEOL (JEOL JSM-550, Japan) (Tawfeek et al. 2020).

Drug content determination

For determining the exact extract content of the silver NPs, different dilutions (100, 50 or 10uL) of the formula were dissolved separately in 1mL of ethanol to be injected into the HPLC. Standard dilutions of the provided extract were dissolved in ethanol to prepare the standard calibration curve of the extract content. Samples and standards were tested using HPLC at wavelength= 274nm (Table 1).

Table 1: The assessment of drug content and concentrations across various dilution factors highlights the importance of comprehensive testing and validation in pharmacology

Area	451333	227922	43357	42065	41045
Dil. Factor	10	50	100	100	100
Conc (µg/mL)	844.35	414.8139	59.96309	57.47904	55.51796
Actual conc (µg/mL)	8443.5	20740.69	5996.309	5747.904	5551.796
The average			5.7±0.23	mg/ml	

HPLC method

The samples were tested using HPLC at wavelength=274nm. HPLC analysis conditions: Injection volume: 10µL, Wavelength: 274nm, Column inertsil C18: 4.6x250mm, 5µm, Mobile phase: Acetonitrile: water (50:50), Mode of elution: Isocratic, Flow rate: 1mL/min, Temperature: 30°C (Hajimehdipoor et al. 2010).

Animals and groups

Twenty-four adult healthy male Barbary goats were included in this study for experimental procedures. Their ages were 12 to 18 (mean, 13±1.5) months, and their weight were from 18–25, (mean, 21±0.5) kg. Studied goats were confined in suitable acceptable stall with a suitable temperature of 27±0.5°C and humidity of 55±0.4%. They received feeding, water and received human care according to Institutional Animal Care Guidelines. Surgery was carried out in all goat's groups to induce a 3.5mm in diameter bone defect at the middle third of both right third metacarpus in each goat. In group 1 (n=12) (*Thymus vulgaris* extract) had injected with *Thymus vulgaris* extract liquid at the bone defect, group 2 (Ag-NPS THV) (n=12) had injected with Ag-NPS *Thymus vulgaris* liquid injection at the bone defect.

Surgical procedure

Routine clinical evaluations were carried out for goats before surgery, as well as fasting of the studied animals was performed for 12 hours preoperatively. Penicillin-streptomycin, (Norbrook Laboratories, Newry, UK) was administrated (IM) at a dose of 10,000 IU/kg for the penicillin and 5mg/kg streptomycin and flunixine meglumine, (Schering-Plough, Welwyn Garden City, Hertfordshire, UK) at 1.1mg/kg was done preoperatively. Animals were sedated by IV injection of xylazine HCl (Seton 2%), (Laboratorios Calier, S.A., Barcelona, Spain) at dose of 0.05mg/kg. The goat was placed in lateral recumbency, followed by clipping and aseptic preparation of the lateral aspect of both metacarpal and metatarsal regions, local infiltration analgesia was performed using lidocaine HCl (lidocaine hydrochloride 2%), (Norbrook Laboratories, Newry, UK). following anesthesia; skin incision (1cm) was created approximately at the middle third of the cannon region where bone exposed and 3.5mm bone defect was made only on the lateral cortices and not reaching the medial ones (Fig. 1A). The drilling of the bone was performed in a mediolateral direction using a 3.5mm diameter drill bit. Following drilling, the surgical site was flushed with sterile normal saline, and skin was closed by single interrupted horizontal mattress using braided Silk No.1 (SMI, Steinberg, Belgium). Then, animals in group 1 and group 2 were injected at the bone defect with 1mL *Thymus vulgaris* extract and Ag-NPs *Thymus vulgaris* liquid, respectively. Pressure bandages were applied and changed day after day for 5 times. *The sutures* were removed at 10th day post-surgery. The preoperative antibiotic and anti-inflammatory drugs were continued for 4 successive days after surgery, and the surgical site was evaluated for infections and swelling.

Radiographic assessment

Radiological evaluation of bone healing process of metacarpal bone defect was performed beginning from 0 day post-operatively and every two weeks for 8 weeks using X-ray apparatus (Toshiba, Japan) 48KV, 0.7mAs, with focal film distance of 70cm. Two Standard radiographic views including; dorsopalmar and lateromedial views were obtained for each operated goat. All obtained radiographic views were precisely assessed at different times points until complete healing of the bone defect. Scoring of bone radiographs was assessed using the modified RUS system graded from 1 to 4 grades as follows; visible fracture line and absent callus (score 1), visible fracture line and visible interrupted callus (score 2), invisible fracture line and visible bridging callus (score 3), no fracture line and no callus (score 4). The scores of all cortices were then combined to give a minimum score of 4 (definitely not healed) and a maximum of 10 (completely healed) according to Leow et al. (2016).

IJVS Press

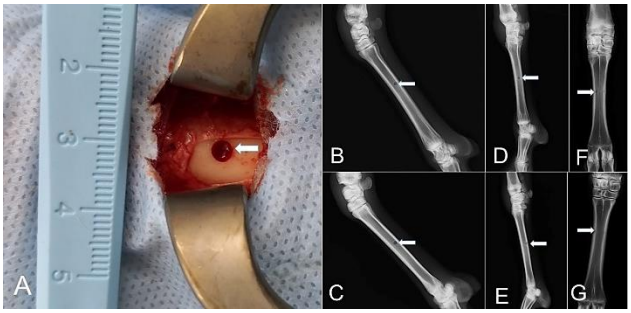

Fig. 1: Skin incision at the medial aspect of the middle third of the right metacarpal with the creation of 3.5mm bone defect (A), immediate postoperative lateral radiographs of bone defect at metacarpal + THV-liquid (group 1) (B), bone defect at metacarpal + AgNPs-THV (group 2) (C). Postoperative (day 42) lateral radiographs of bone defect at metacarpal + THV-liquid (group 1) (D), bone defect at metacarpal + AgNPs-THV (group 2) (E). Postoperative (day 56) dorsopalmar radiographs of bone defect at metacarpal + THV-liquid (group 1) (F), bone defect at metacarpal + AgNPs-THV (group 2) (G).

Blood sampling and laboratory analysis

For evaluation of bone turn over biomarkers, blood samples were collected from the jugular vein from each studied rabbit into plain vacutainer tubes using an 18-gauge, needle (Mais Co., Saudi Arabia). These samples were collected on 0 days (pre-operative) and at every two weeks for eight weeks postoperatively to assess the progression of healing process of metacarpal bone defect among the treated rabbits. The blood samples were centrifuged at 4500rpm for 15min to obtain clear serum; then sera were preserved and freeze at -20ºC. Sera was used to assess the level of calcium and phosphorus using laboratory kits (Mybiosource, USA) and spectrophotometry techniques, according to Tharwat (2020), Sakhaee et al. (2024) and Zillinger et al. (2024).

Histopathological evaluation

The right metacarpal bone was taken from each goat for histopathological evaluation. Firstly, bones were dissected and the soft tissues were removed. About 1cm up and down of the cross-section of the bone defect region was cut by a moderate speed saw and directly immersed in a plenty of fixative10% neutral buffered formalin solution. After fixation, the bones samples were decalcified in 15% buffered formic acid solution. The samples were then embedded in paraffin-embedding technique. Two sections of 5µm thickness were taken from the center of each specimen, then stained with hematoxylin and eosin. The healing process were evaluated, reviewed and scored blindly by two pathologists using Huo et al. (1991).

Clinical study

Animals

Forty-nine animals (sheep, n=36; goats, n=13) suffering from various types of metacarpal and metatarsal bone fractures were examined in this study over the period of 2023–2024 at University Veterinary Hospital, Qassim University, Saudi Arabia. There were 13 male and 23 female sheep of different three local breeds (Naimi, Nagdi, and Sakni), with age ranging from one to 70 (mean, 32±17) months and weight ranging from 15 to 65 (mean, 35±16) kg. There were 3 male and 10 female goats of two breeds (Syrian and Baladi), aged between one and 66 (mean, 33±16) months and weighing between 12 and 63 (mean, 35±15) kg. All animals underwent a thorough physical examination.

Clinical examination

At admission, sheep and goats were assessed clinically and subjectively for metacarpal and metatarsal bone fracture. Body temperature and vital signs were reported for every sheep and goat. Data about each sheep and goats involved in this study, which include age, breed, sex, were assessed, compared, and statistically analyzed.

Radiographic examination

Dorsopalmar or dorsoplantar and lateromedial standard radiographic views were performed for each affected sheep and goat (Fig. 2A) using Minx ray HF 100/30 generator (Toshiba, Tokyo, Japan), according to Kofler et al. (2017) Light sedation of the examined sheep and goats was performed using 0.05 mg/kg xylazine HCl 2%, intravenously injected (IV). All radiographic views were subjectively evaluated before surgical intervention and all examined sheep and goats were routinely treated with external fixation (Fig. 2B and C).

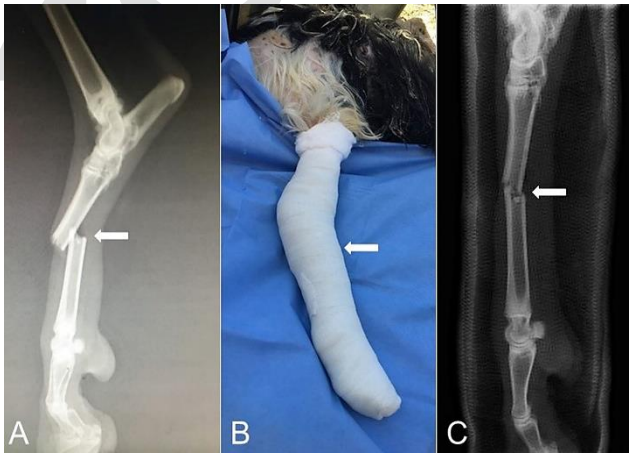

Fig. 2: A. Lateral radiograph of complete single transverse diaphysial metatarsal fracture in sheep (arrow). B. External fixation using gibsona (arrow). C. Lateral radiograph post external fixation of complete single diaphysial metatarsal fracture in sheep (arrow).

Statistical analysis

In this study, SPSS for Windows (Version 21.0) was used to run our data analysis. Data were assessed for normality distribution using D'Agostino-Pearson test. As data were found normally distributed, mean and standard deviation for each variable were presented. To assess the effect of treatments on the mineral levels and radiographic scores, general linear model (GLM) with repeated measure ANOVA was used. In this test, the result of Wilks Lambada was used to assess the effect of time and time -treatment interaction. As this test was found significant, unpaired t-test was used to assess the significant effective treatment at each time point. To evaluate the effect of treatment on the histopathological findings, Fishers exact test was used. At p-value of < 0.05, the result was considered significant.

In Press

RESULTS

Experimental study

During the first 2 weeks in both groups, all animals were normal and did not suffer any clinical disorders. Lameness was detected at 14th day only in one goat (Ag-NPs-THV group), while THV group showed no lameness. Wound dehiscence was detected in one animal of THV group with exposure of bone defect and exudation which was treated by local antiseptic spray and bandaging (healing occurred after one week). Calluses were clinically palpated at 2 weeks in one and three goats in THV and Ag-NPs-THV groups, respectively.

Preparation and characterization of AgNPs-THV

The AgNPs-THV were synthesized through the reduction technique. It is synthesized as a clear solution without any aggregation. The formed AgNPs-THV were synthesized through the reduction of AgNO3 using the extract of THV as a reducing agent. The formed AgNPs-THV were formed after conversion the colour from yellow colour of the THV extract to buff-red after formation of AgNPs-THV. The average particle size of AgNPs-THV was recorded at 1233±175nm. The polydispersity index (PDI) of 0.528 is low, indicating that the sample has a narrow particle size distribution. A low PDI is required for consistent behaviour in both stability and biological interactions, making AgNPs-THV more promising for future applications. The nanoparticles have a Zeta Potential of -18.1±1.74mV, indicating good stability in dispersions. A zeta potential value above ±30mV indicates high stability, while levels approaching zero indicate vulnerability to aggregation. Thus, whereas AgNPs-THV exhibit reasonable stability, more modifications or functionalization may be required to improve their lifespan in a variety of applications (Fig. 3A). Throughout the experimental process of AgNPs-THV, upon the addition of THV to AgNO3, a colour change was observed. The formed AgNPs-THV was primarily yellowish, and upon further heating, the colour changed to dark brown as the solution was kept boiling for 15min. The AgNPs-THV free electrons generated the SPR resonance bands (Ranoszek-Soliwoda et al. 2017). The UV-VIS spectra of AgNPs-THV showed a redshift in the surface plasmon resonance peak for all the produced AgNPs-THV. The obtained colors had wavelength of 381.5±2.1, 388.5±2.2nm for THV and AgNPs-THV, respectively (Fig. 3B). The transmission electron microscope (TEM) detected oval nanoparticles with a size of 50nm. The nanoparticles' comparatively large size suggests that they may exist in aggregates or clusters. While greater sizes can alter the efficacy of AgNPs in biological applications, particular performance must be assessed in context. The TEM image (Fig. 3C) shows that the AgNPs-THV display oval, round, and clustering (green arrow) behavior, indicating that aggregation may occur because of unnecessary extract or silver nitrate concentrations during synthesis. In contrast, the TEM images show a more focused view, exhibiting nanoparticles resembling a nucleus coated (red arrow) in an outer layer of THV extract (blue arrow) (Fig. 3D). This finding is especially relevant since it implies that the coating serves an important role in stabilizing the nanoparticles and improving their functionality. The inclusion of the plant extract not only helps to keep nanoparticles at the right size, but it also imparts additional qualities that may improve their utility in biological applications (Abdellatif et al. 2024; Sadan et al. 2024).

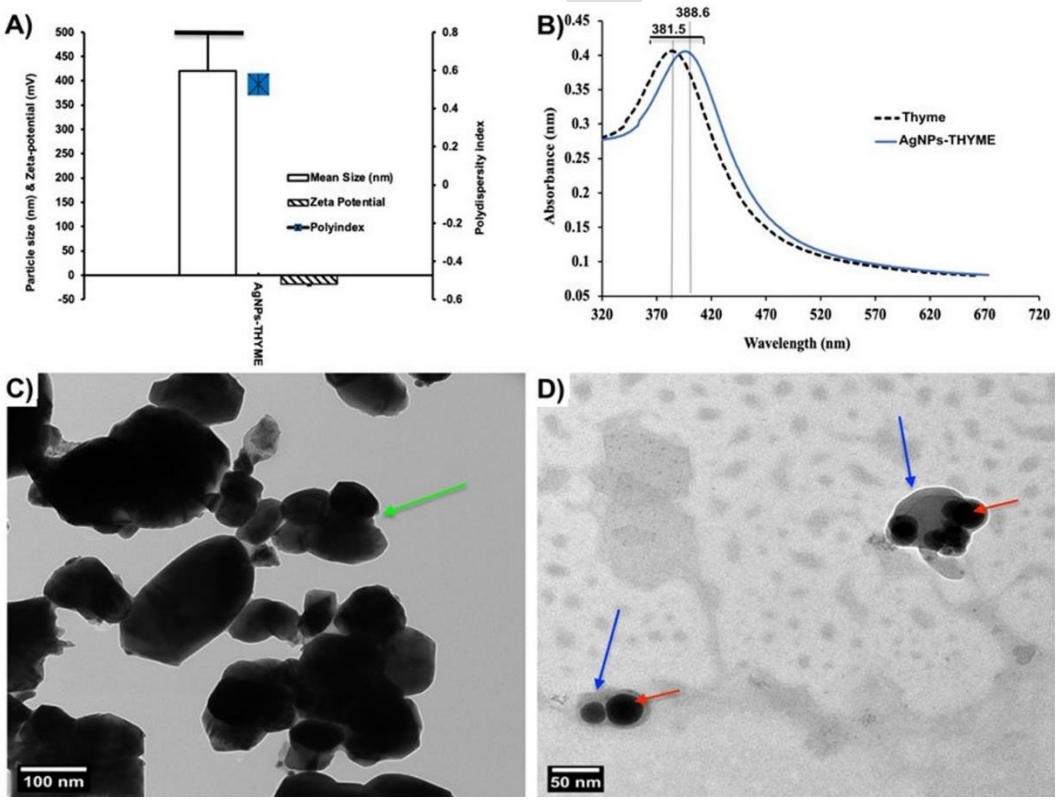

Fig. 3A): The size in diameter and zeta-potential of the prepared AgNPs-THV as determined by dynamic light scattering. B) UV-VIS of THV extract and AgNPs-THV. C) Transmission electron microscope of the silver nanoparticles reduced with THV as particles showed at clusters and aggregated while D) focusing of the NPs which showed as nucleus coated with outer layer of plant extract.

Moreover, the amount of THV was determined using HPLC method. The results showed drug concentrations at different dilution factors (10, 50, 100, 100 and 100), exemplified as areas (451333, 227922, 43357, 42065, and 41045). The obtained conc in µg/mL were as follows (844.35, 414.8139, 59.96309, 57.47904 and 55.51796). To give more context, the data were processed to determine the average concentration, which was 5765.336µg/mL. Moreover, an important statistical indicator, SD was measured at 222.7685µg/mL. This reveals the consistency and dependability of the measures gathered. A reduced SD indicates that the concentrations are closely related to the average, signifying excellent dependability in the experimental method.

Additionally, as drugs undergo formulation changes, understanding how these alterations affect concentrations is vital. For instance, changes may arise due to excipients used, pH levels, temperature, or other environmental factors. Therefore, consistent monitoring and analysis, as performed in this study, are essential for maintaining drug integrity and efficacy.

Radiographic findings

The radiographic union scale was significantly affected by treatment and time (Wilks Lambda test for treatment x time interaction, (P<0.001). AgNPs-THV significantly provided better radiographic union scale than that provided by THV Extract at 2, 5 and 8 weeks post treatment. Thus, the radiographic union score for AgNPs-THV and THV Extract were (1.83±0.40 vs 1.16±0.40), (3.66±0.51 vs 2.16±0.40) and (9.66±0.81 vs 8.33±0.81) at 2, 5, and 8 weeks post treatment (Fig. 4).

BTMs findings

There was significant effect of time and treatments on the level of serum calcium (Walk's, Lambda test for time, P=0.00; and for treatment x time interaction, P=0.02). Serum calcium was significantly increased in AgNPs-THV group in comparison with THV extract group (Fig. 5). Similarly, the effect was recorded for the serum phosphorus level. Where, the level of phosphorus was significantly decreased in AgNPs-THV group in comparison with THV extract group at the 6th week post-treatment (Fig. 6).

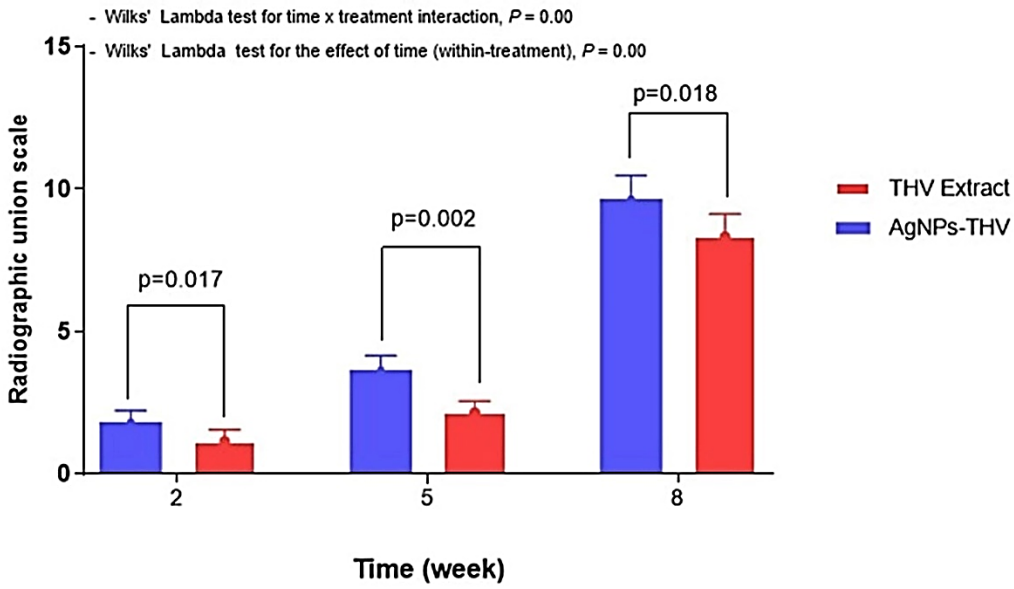

Fig. 4: Comparative effect of Thymus vulgaris extract (THV Extract) and Silver Nanoparticles of Thymus vulgaris (AgNPs-THV) on radiographic union scale in goats with experimentally induced bone defect. The P-value for the difference between the two treatments at the different time points is presented.

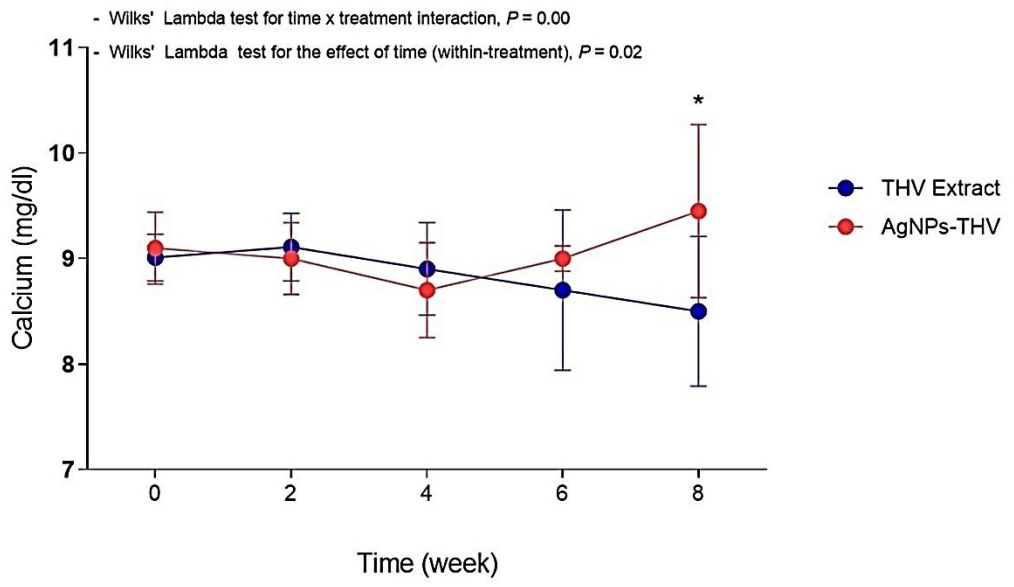

Fig. 5: Comparative effect of Thymus vulgaris extract (THV Extract) and Silver Nanoparticles of Thymus vulgaris (AgNPs-THV) on serum calcium in goats with experimentally induced bone defect. *: indicate the significant variation between the treatments at the corresponding time point.

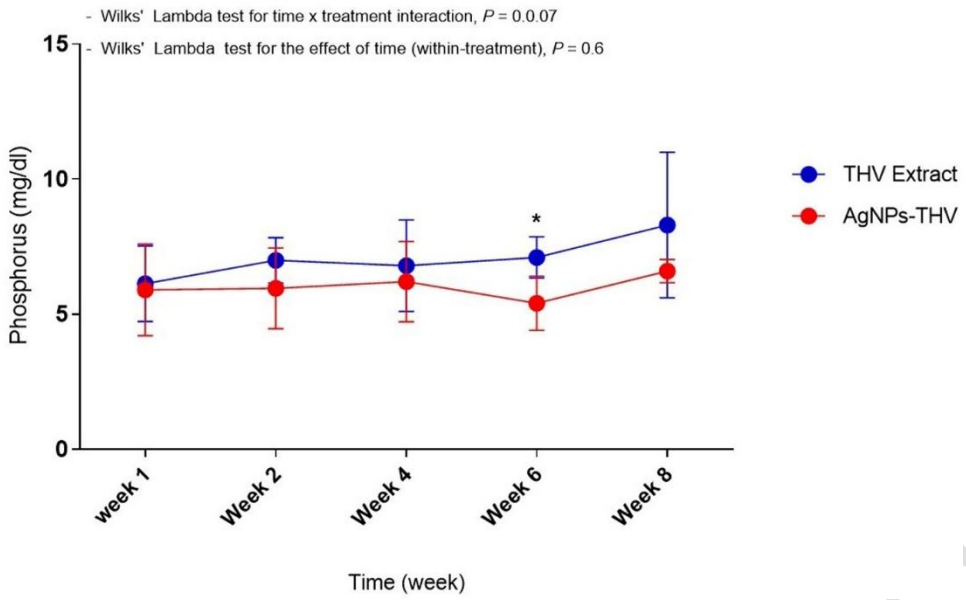

Fig. 6: Comparative effect of Thymus vulgaris extract (THV Extract) and Silver Nanoparticles of Thymus vulgaris (AgNPs-THV) on serum Phosphorus in goats with experimentally induced bone defect. *: indicate the significant variation between the treatments at the corresponding time point.

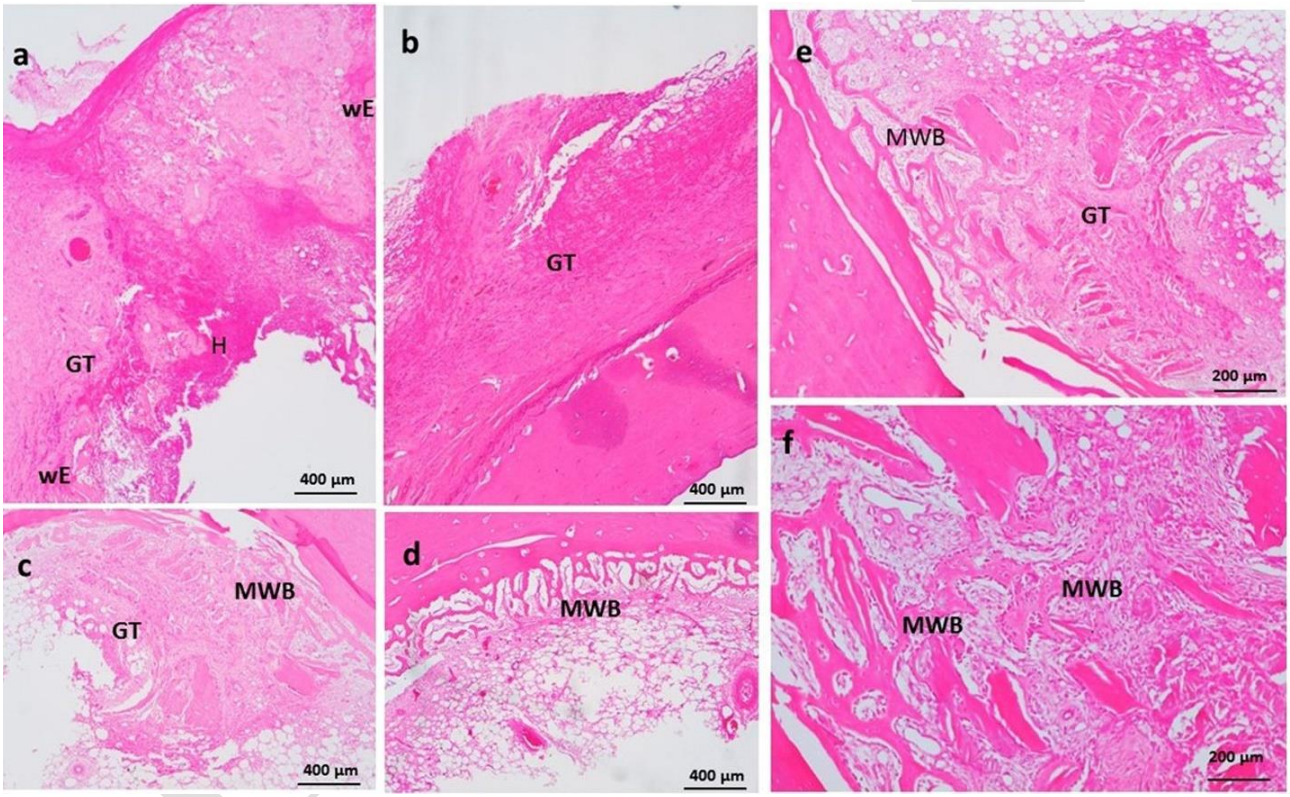

Fig. 7: Empty gap filled mostly with granulation tissue at the site of bone defect at 2 weeks post-operative in extract of Thymus vulgaris group (a). In contrast, granulation tissue (b) and minimal immature bone formation (Woven cancellous bone) with higher medullary (c and d) and periosteal woven bone formation were observed in silver nanoparticles of Thymus vulgaris group. Moreover, granulation tissue, inflammation lysis of bone was observed more prominent in extract group (Fig. e) in comparison to nano group where medullary woven bone formation was prominent (Fig. f).

Histopathological findings

Histopathological examination revealed surgical empty gap filled mostly with granulation tissue in bone defect site at the 2nd week post-operation in THV Extract group (Fig. 7A). In contrast, granulation tissue (Fig. 7B) and minimal immature bone formation (Woven cancellous bone) with higher medullary (Fig. 7C and D) and periosteal woven bone formation were observed in Ag-NPs-THV group. Moreover, granulation tissue, inflammation lysis of bone was observed more prominent in THV Extract group (Fig. 7E) in comparison to nano group where medullary woven bone formation was prominent (Fig. 7F). At the 5th week post-operation, all cases in THV Extract group still have fracture gap filled with woven cancellous bone, cartilage and fibrovascular tissue (Fig. 8A, B). In contrast, mature lamellar bone with woven callous formation filled the fracture gap in Ag-NPs-THV group (Fig. 8C, D). Mature lamellar bone formation was observable at the 8th week post-operation in all animals of Ag-NPs-THV group (Fig. 9C, D), but mature lamellar bone was observed in

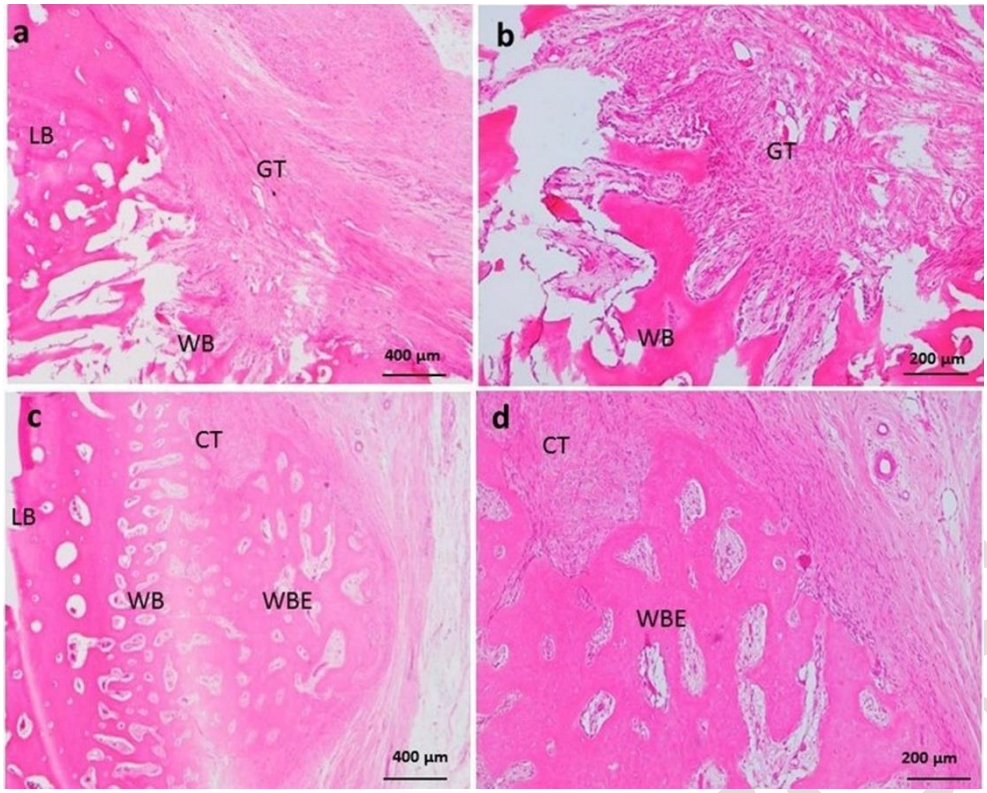

Fig. 8: At the 5th week post-operation, all cases in extract group still have wound gap filled with woven cancellous bone, cartilage and fibrovascular tissue (Fig. a, b). In contrast, mature lamellar bone with woven callous formation filled the wound gap in nano group (Fig. c, d).

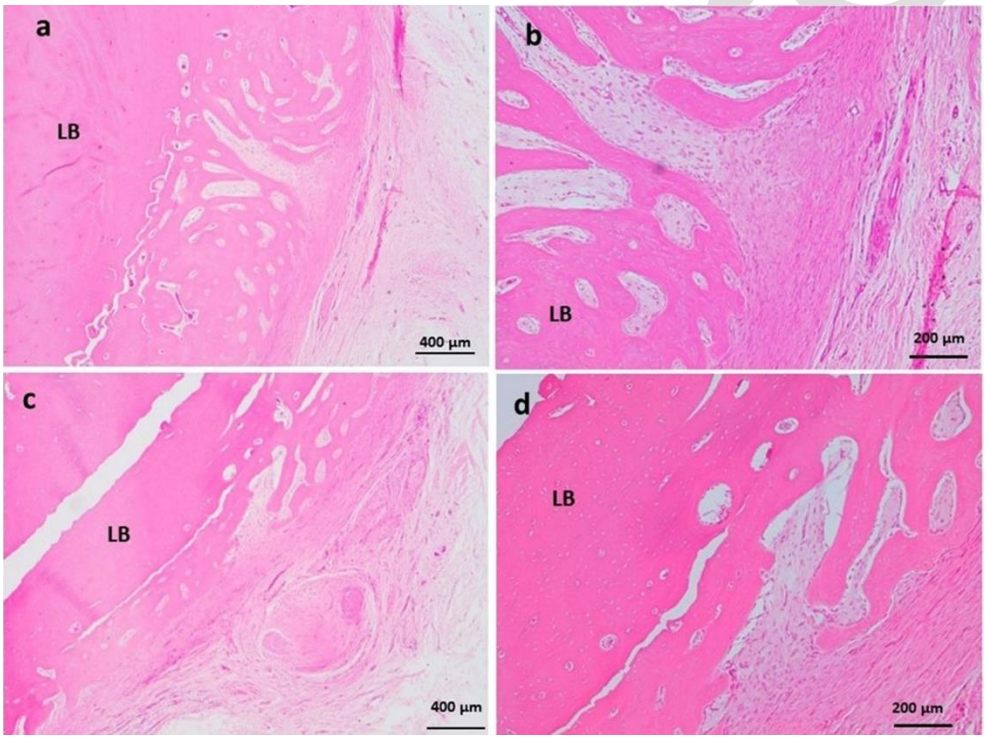

Fig. 9: Mature lamellar bone formation was observable at the 8th week post-operation in all animals of nano group (c, d), but mature lamellar bone was observed in only 2 animals in extract group (a, b).

only 2 animals in THV Extract group (Fig. 9A, B) and others two cases had incomplete bone healing (fracture and callous formation). The incomplete calcification was prominent in cases of THV Extract in comparison with those of Ag-NPs-THV group).

Histopathologically, at five weeks post-operative, Ag-NPs-THV treated group showed a significant decrease in fracture gap that filled with woven bone beside lamellar bone in comparison with THV Extract group ($P<0.01$) that still had wider gap filled with granulation tissue and limited woven bone. Thus, Ag-NPs-THV provided rapid healing response than THV Extract only (4/4 vs 0/4). At eight weeks post-treatment, 100 % of cases treated with Ag-NPs-THV showed complete healing with lamellar bone compared with 50% of THV Extract treated group (4/4 vs 2/4), (Table 2).

Clinical study

Clinical findings

Forty-nine animals (36 sheep and 13 goats, 42.6%) were clinically diagnosed with metacarpal and metatarsal bone fractures out of 115 fracture cases admitted to the University Veterinary Hospital, Qassim University, Saudi Arabia during the study period. Out of 36 studied sheep,

Table 2: Summarizes the healing process of induced fracture in metacarpal bone in goats after treatment with extract and silver nanoparticles of *Thymus vulgaris*

Time	*Thymus vulgaris* Extract (THV Extract) group	Silver nanoparticles of *Thymus vulgaris* (AgNPs-THV) group
At 2 weeks post operation	Fracture gap filled with granulation tissue and remnant of hematoma. Periosteal and medullary woven bone formation associated with necrotic bony spicules and granulation tissue	Fracture gap filled with granulation tissue. Higher periosteal and medullary woven bone and minimal inflammation
At 5th week post-operation	(4l4) Fracture gap still have granulation tissue, cartilage, and woven bone	(0/4) Fracture gap contain granulation tissue and (4/4) Fracture gap filled with woven bone beside lamellar bone.
At 8 weeks post-operation	(2/4) complete healing with lamellar bone	(4/4) complete healing with lamellar bone

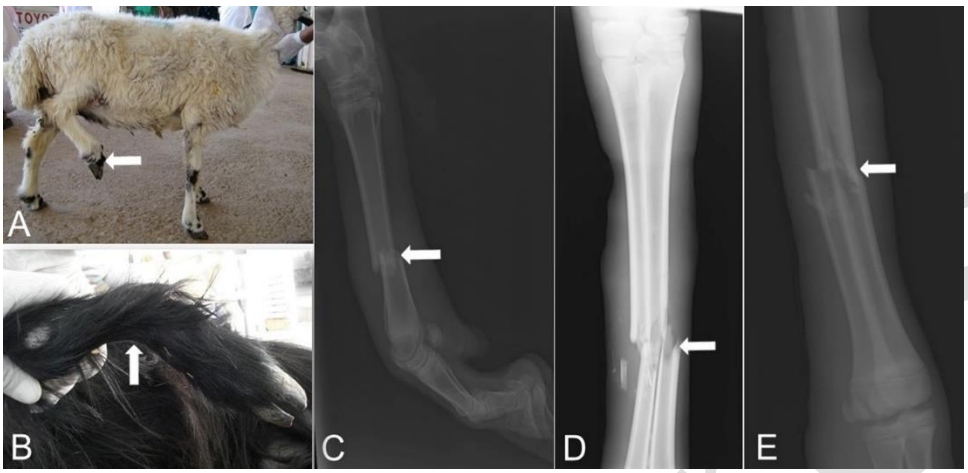

Fig. 10: A. Complete inability of weight bearing on the right hind limb in sheep due to metatarsal fracture (arrow). B. Deformity of the forelimb in a goat in picture (arrow). C. Lateral radiograph of complete metatarsal fracture in sheep (arrow). D. Dorsopalmar radiograph of complete multiple transverse diaphysial metacarpal fracture in sheep (arrow). E. Dorsopalmar radiograph of impacted displacement of metacarpal fracture in sheep (arrow).

metatarsal (n =22; 61.1%) were more prevalent than metacarpal (n =14; 38.9%) fractures. Prevalence of both fractures was higher in female (n =23; 63.9%) than male sheep (n = 13; 36.1%).

Out of 13 studied goats, metacarpal and metatarsal prevalence was higher in female (n=10; 76.9%) than male goat (n=3; 23.1%). As well as, fracture prevalence was greater in metatarsus (n=8; 61.5%) than metacarpus (n=5; 38.5%).

The affected sheep and goats with metacarpal and metatarsal bone fractures showed pain, swelling, inability to bear weight (Fig. 10A), deformity (Fig. 10B), crepitation, and abnormal mobility of the fractured part.

Radiographic findings

Radiography of metacarpal and metatarsal bone fractures in the affected sheep and goats were carried out, it revealed radiolucent line, providing evidence of swelling of the surrounding soft-tissue on the lateral radiographic view (Fig. 10B, C and D), with the presence of oblique or transverse fracture lines with or without displacement of bone fragments (Fig. 10D). The fractures were single (Fig. 10C), multiple (Fig. 10D) or comminuted at different locations; diaphysial, metaphyseal and epiphyseal.

DISCUSSION

Thymus vulgaris has essential oils such as Thymol, which has antibacterial, antifungal and antiseptic properties (Aljabeili et al. 2018; Diniz et al. 2023). The extract contains various phytochemicals that act as reducing and stabilizing agents for the silver nanoparticles. The synthesized silver nanoparticles using Thymus vulgaris have various applications in the field of medicine (Abdelhamed et al. 2022; Taha et al. 2024; Al-Rimawi et al. 2024). They have antibacterial, antifungal, and antiviral properties, making them an excellent candidate for treating various infections. The nanoparticles can also be used as a drug delivery system, where the drug is loaded onto the surface of the nanoparticles and delivered to the target site (Al-Rimawi et al. 2024; Taha et al. 2024). This reduces the amount of drug required and enhances the therapeutic effect. Several studies have investigated the potential use of green synthesized silver nanoparticles using *Thymus vulgaris* in wound healing and bone fracture. One study found that silver nanoparticles synthesized using *Thymus vulgaris* extract could promote wound healing in rats by increasing the rate of epithelialization and reducing the inflammatory response. Another study showed that silver nanoparticles synthesized using *Thymus vulgaris* extract could enhance the healing of bone fractures in rats by increasing bone mineral density and improving bone microarchitecture (Antih et al. 2021; Alsakhawy et al. 2022). The obtained results show that AgNPs coated with THV extract have an average particle size of 1233nm and a standard deviation of ± 175.5nm, demonstrating significant variation in particle size. Larger particles may have different properties and applications than their smaller counterparts.

The absorption is a sign of the size, responsiveness, and the SPR of the nanoformulations (Abdellatif et al. 2018; Abdellatif 2020). The AgNPs-THV displayed a distinctive engagement peak at ~388.5nm due to the presence of free electrons which produce the significance of the SPR band (Ranoszek-Soliwoda et al. 2017). The UV-VIS spectra showed a ongoing redshift in the SPR and the peak absorption which were qualified to the permanent increase in the sizes of AgNPs-THV due to the coating with THV (Steinigeweg and Schlucker 2012). Notably, we have used TEM to see oval nanoparticles of roughly 50nm,

demonstrating the intricacy and variability in particle morphology that can arise throughout the synthesis process. The difference in particle size reflects the synthesis method's efficiency and processing conditions. Tiny nanoscale often has a higher surface-to-volume ratio, which can lead to increased reactivity and improved performance in applications like drug delivery, where targeting and cellular interaction are crucial (Aldosari et al. 2023; El-Readi et al. 2024). Larger AgNPs, on the other hand, may be better suited for applications requiring stability and lifespan in a variety of situations, such as antibacterial coatings for healthcare items. The use of THV as a stabilizing agent is significant for several reasons. THV contains phenolic chemicals, flavonoids, and essential oils with antioxidant effects. These compounds not only aid to reduce silver ions and generate silver nanoparticles, but they also give the particles stability and avoid agglomeration. This stabilization is critical for keeping the nanoparticles intact during storage and application (Diniz et al. 2023).

Metacarpal and metatarsal fractures are common occurrence in sheep and goats. They represent one of the most frequent emergencies for surgical treatment. However, there is limited literature available about the diagnosis and treatment of metacarpal and metatarsal bone fractures. Thus, the present research was designed to assess metacarpal and metatarsal fractures in sheep and goats and to describe the accelerating action of silver nanoparticles *Thymus vulgaris* (Ag-NPs-THV) on fracture healing in goats (experimental study). In the examined sheep and goats, metacarpal and metatarsal bone fractures were more common in sheep than goats. This may be due to high number of the sheep in comparison to goats in Saudi Arabia in relation to its productive and reproductive values (Boshra et al. 2015). The affected sheep and goats with metacarpal and metatarsal bone fractures showed pain, swelling, inability to bear weight, deformity, crepitation, and abnormal mobility of the fractured part. This finding was in coinciding with (Lozier et al. 2018). Forty-nine animals (36 sheep and 13 goats, 42.6%) were clinically diagnosed with metacarpal and metatarsal bone fractures out of 115 fracture cases admitted to the University Veterinary Hospital, Qassim University, Saudi Arabia during the study period. The Case history, clinical and radiographic findings of metacarpal and metatarsal bone fractures in sheep and goats are routinely done for the diagnosis of this affection in such animals (Lozier et al. 2018).

Cellular, biomechanical, hormonal, and pathological mechanisms have been controlled the healing process of bone fractures or injuries after their occurrence (Sadan et al. 2024). Although regeneration of fractures is physiological mechanism, different techniques have been applied to enhance the regeneration and healing of the bone fractures. Medicinal plants have been used in several researches to accelerate bone regeneration (Sadan et al. 2024; Sadan et al. 2025). Collaboration between different diagnostic tools including RUS, BTMs, and histopathological findings was used in our study as a unique assessment techniques of fracture repair. Our finding was in accordance with Al-Sobayil et al. (2020); Sadan et al. (2024) and Sadan et al. (2025). Post-operative radiological evaluation (≤ 8 weeks) showed that, the radiographic union scale was significantly affected by treatment and time (Wilks Lambda test for treatment x time interaction, $P<0.001$. AgNPs-THV significantly provided better radiographic union scale than that provided by THV Extract at 2, 5 and 8 weeks post treatment. Turnover biomarkers of bone healing process have been used in different researches for investigation and evaluation of the bone healing and regeneration, and it has been considered as a unique diagnostic technique for monitoring and following up of fracture regeneration (Sadan et al. 2024; Sadan et al. 2025). Measuring of bone turnover biomarkers during the healing of bone fractures and injuries could give informative evaluation of bone healing progress, and help for proper surgical decision (Al-Sobayil et al. 2020). Serum calcium was significantly increased in AgNPs-THV group in comparison with THV extract group. Similarly, the effect was recorded for the serum phosphorus level. Where, the level of phosphorus was significantly decreased in AgNPs-THV group in comparison with THV extract group at the 6th week post-treatment. This might be contributed to calcium and phosphorus effect on regeneration and maturation of bone as recorded by Sadan et al. (2024) and Sadan et al. (2025).

In the present study, *Thymus vulgaris* enhanced bone healing through induction of granulation tissues formation as well as periosteal and medullary woven bone formation that filled the fracture gap and the later increased gradually to replace the granulation tissue with woven bone that lastly remodelled to lamellar bone. Previously administrating *Thymus vulgaris* ointment, significantly increased fibroblast and macrophages distribution and up-regulated the new vessels formation and collagen deposition on days 3, 7, 14 and 21 after wound induction (Panah et al. 2014). Beside the antibacterial activity of thymol and enhancement of healing, incorporating thymol into the dressing of wounds increases its elasticity and porosity, but reduces its mechanical strength (Mollarafie et al. 2015). Thymus oil serve as a protective agent to the burned tissues by decreasing the NO level and enhanced burn healing by induction of new tissue formation (Dursun et al. 2003). The acceleration of healing after application of thyme might be due to thyme essential oils that have antibacterial and antioxidant activities (Aljabeili et al. 2018). All previous works of thyme extract applications are on soft tissue healing including surgical wounds and burns. No previous work on role of thyme on healing of bone fracture. The present work elucidated that Thyme extract or nanoparticles help in induction of bone fracture healing. A previous study in role of thyme to prevent osteoporosis was conducted. Thyme and rosemary supplementation significantly hindered the development of bone loss, elevated Ca and vitamin D3 in plasma, improved bone mineral density and counteracted the oxidative stress and inflammation (improved TNF-α, C-reactive protein and MDA) in comparison to the low-calcium osteoporotic control. Moreover, bone histology and protection against bone loss were improved and powder of thyme was more effective than rosemary (Elbahnasawy et al. 2019). Similarly, Thyme increased the osteogenesis, bone mineral density and remodelling of bone tissue. In a trial for the best utilization of thyme extract, it was co-loaded with ginger to polyvinyl alcohol and chitosan electrospun nanofibers for tackling infection and wound healing promotion (Maleki et al. 2024).

The loaded mat had high wettability, porosity and liquid absorption capacity without any adverse interaction as well as a high antioxidant activity and antibacterial effect. The loaded mat significantly accelerated cutaneous wound healing in bacterial-infected rats by preventing bacteria growth at the wound site and induction of collagen fibers and appendages formation and in turn skin regeneration. Overall, the mat containing ginger-thyme extracts provides a promising effect for inhibiting wound infection and accelerating the healing process (Maleki et al. 2024). Similarly, in the present study thyme extract was applied as crude extract and as sliver nanoparticles loaded extract. The nanoparticle form accelerated the fracture healing than crude extract as observed in more woven bone formation at the 5th week post-operation as well as complete healing of all cases treated with nanoform corresponding to 50% of cases treated with crude extract. thyme nanoparticles form exhibited higher antioxidant and antibacterial activities than crude extract (Aldosary et al. 2021). Moreover, the anti-inflammatory property as well as antibacterial activity of nanoparticles of thyme were higher than of standard extract (Heidari et al. 2018; Pandiyan et al. 2022). anti-inflammatory, antidiabetic and antioxidant effects of sliver nanoparticles of thyme were higher than those of extract were also observed in a recent study (Ejaz et al. 2024).

Funding: The authors gratefully acknowledge Qassim University, represented by the Deanship of Scientific Research, on the financial support for this research under the number (2023-SDG-I-HMSRC-35984) during the academic year 1445 AH / 2023 AD".

Conflict of Interest: The authors declare no conflicts of interest.

Data Availability: All data supporting the findings of this study are available within the manuscript and no additional data sources are required.

Author's Contribution: MS and AA concept and designed the proposal. MS, and WR performed the experimental section. AA performed the *Thymus vulgaris* extract and *Thymus vulgaris* silver nanoparticles. MH performed and evaluated the histopathological examinations. MS and WR performed the laboratory analysis. WR analyzed the data statistically, and MS, AA, MH, AH and WR analyzed and interpreted the data. All authors revised and approved the final manuscript.

Generative AI Statement: The authors declare that no Gen AI/DeepSeek was used in the writing/creation of this manuscript.

Publisher's Note: All claims stated in this article are exclusively those of the authors and do not necessarily represent those of their affiliated organizations or those of the publisher, the editors, and the reviewers. Any product that may be evaluated/assessed in this article or claimed by its manufacturer is not guaranteed or endorsed by the publisher/editors.

REFERENCES

Abdelhamed FM, Abdeltawab NF, ElRakaiby MT, Shamma RN and Moneib NA, 2022. Antibacterial and anti-inflammatory activities of *Thymus vulgaris* essential oil nanoemulsion on acne vulgaris. Microorganisms 10(9): 1874. https://doi.org/10.3390/microorganisms10091874

Abdellatif AA and Tawfeek HM, 2016. Transfersomal nanoparticles for enhanced transdermal delivery of clindamycin. American Association of Pharmaceutical Scientists 17(6): 1507. https://doi.org/10.1208/s12249-015-0441-7

Abdellatif AAH, Abou-Taleb HA, Abd El Ghany AA, Lutz I and Bouazzaoui A, 2018. Targeting of somatostatin receptors expressed in blood cells using quantum dots coated with vapreotide. Saudi Pharmaceutical Journal 26(8): 1162-1169. https://doi.org/10.1016/j.jsps.2018.07.004

Abdellatif AAH, 2020. A plausible way for excretion of metal nanoparticles via active targeting. Drug Development and Industrial Pharmacy 46(5): 744-750. https://doi.org/10.1080/03639045.2020.1752710

Abdellatif AAH, Rasheed Z, Alhowail AH, Alqasoumi A, Alsharidah M, Khan RA, Aljohani ASM, Aldubayan MA and Faisal W, 2020. Silver citrate nanoparticles inhibit PMA-induced TNFalpha expression via deactivation of NF-kappaB activity in human cancer cell-lines, MCF-7. International Journal of Nanomedicine 15: 8479-8493. https://doi.org/10.2147/ijn.s274098

Abdellatif AA, Alturki HN and Tawfeek HM, 2021a. Different cellulosic polymers for synthesizing silver nanoparticles with antioxidant and antibacterial activities. Scientific Reports 11(1): 84. https://doi.org/10.1038/s41598-020-79834-6

Abdellatif AAH, Alsharidah M, Al Rugaie O, Tawfeek HM and Tolba NS, 2021b. Silver Nanoparticle-Coated Ethyl Cellulose Inhibits Tumor Necrosis Factor-alpha of Breast Cancer Cells. Drug Design, Development and Therapy 15: 2035-2046. https://doi.org/10.2147/dddt.s310760

Abdellatif AAH, Alhathloul SS, Aljohani ASM, Maswadeh H, Abdallah EM, Hamid Musa K and El Hamd MA, 2022a. Green synthesis of silver nanoparticles incorporated aromatherapies utilized for their antioxidant and antimicrobial activities against some clinical bacterial isolates. Bioinorganic Chemistry and Applications 2022: 2432758. https://doi.org/10.1155/2022/2432758

Abdellatif AAH, Osman SK, Alsharidah M, Al Rugaie O, Faris TM, Alqasoumi A, Mousa AM and Bouazzaoui A, 2022b. Green synthesis of silver nanoparticles reduced with Trigonella foenum-graecum and their effect on tumor necrosis factor-alpha in MCF7 cells. European Review for Medical and Pharmacological Sciences 26(15): 5529-5539. https://doi.org/10.26355/eurrev_202208_29424

Abdellatif AAH, Alhumaydhi FA, Al Rugaie O, Tolba NS and Mousa AM, 2023. Topical silver nanoparticles reduced with ethylcellulose enhance skin wound healing. European Review for Medical and Pharmacological Sciences 27(2): 744-754. https://doi.org/10.26355/eurrev_202301_31077

Abdellatif AAH, Mostafa MAH, Konno H and Younis MA, 2024. Exploring the green synthesis of silver nanoparticles using natural extracts and their potential for cancer treatment. 3 Biotech 14(11): 274. https://doi.org/10.1007/s13205-024-04118-z

Aljabeili HS, Barakat H and Abdel-Rahman HA, 2018. Chemical composition, antibacterial and antioxidant activities of thyme essential oil (*Thymus vulgaris*). Food and Nutrition Sciences 9: 433-446. https://doi.org/10.4236/fns.2018.95034

Al-Rimawi F, Sbeih M, Amayreh M, Rahhal B and Mudalal S, 2024. Evaluation of the antibacterial and antifungal

In Press

properties of oleuropein, olea Europea leaf extract, and *Thymus vulgaris* oil. BMC Complementary Medicine and Therapies 24(1): 297. https://doi.org/10.1186/s12906-024-04596-x

Aldosari BN, Abd El-Aal M, Abo Zeid EF, Faris TM, Aboelela A, Abdellatif AAH and Tawfeek HM, 2023. Synthesis and characterization of magnetic Ag-Fe3O4@polymer hybrid nanocomposite systems with promising antibacterial application. Drug Development and Industrial Pharmacy 49(12): 723-733. https://doi.org/10.1080/03639045.2023.2277812

Aldosary SK, El-Rahman SNA, Al-Jameel SS and Alromihi NM, 2021. Antioxidant and antimicrobial activities of *Thymus vulgaris* essential oil contained and synthesis thymus (Vulgaris) silver nanoparticles. Brazilian Journal of Biology 83: e244675. https://doi.org/10.1590/1519-6984.244675

Alsakhawy SA, Baghdadi HH, El-Shenawy MA, Sabra SA and El-Hosseiny LS, 2022. Encapsulation of *Thymus vulgaris* essential oil in caseinate/gelatin nanocomposite hydrogel: In vitro antibacterial activity and in vivo wound healing potential. International journal of Pharmacology 628: 122280. https://doi.org/10.1016/j.ijpharm.2022.122280

Al-Sobayil F, Sadan MA, El-Shafaey ES and Ahmed AF, 2020. Can bone marrow aspirate improve mandibular fracture repair in camels (camelus dromedarius)? A preliminary study. Journal of Veterinary Science 21(6): e90. https://doi.org/10.4142/jvs.2020.21.e90

Ansar S, Tabassum H, Aladwan NS, Naiman Ali M, Almaarik B, AlMahrouqi S, Abudawood M, Banu N and Alsubki R, 2020. Eco friendly silver nanoparticles synthesis by Brassica oleracea and its antibacterial, anticancer and antioxidant properties. Scientific Reports 10(1): 18564. https://doi.org/10.1038/s41598-020-74371-8

Antih J, Houdkova M, Urbanova K and Kokoska L, 2021. Antibacterial activity of *Thymus vulgaris* L. essential oil vapours and their GC/MS analysis using solid-phase microextraction and syringe headspace sampling techniques. Molecules 26(21): 6553. https://doi.org/10.3390/molecules26216553

Azadi M, Siavash Moghaddam S, Rahimi A, Pourakbar L and Popović-Djordjević J, 2021. Biosynthesized silver nanoparticles ameliorate yield, leaf photosynthetic pigments, and essential oil composition of garden thyme (*Thymus vulgaris L.*) exposed to UV-B stress. Journal of Environmental Chemical Engineering 9: 105919. https://doi.org/10.1016/j.jece.2021.105919

Boshra H, Truong T, Babiuk S and Hemida MG, 2015. Seroprevalence of sheep and goat pox, peste des petits ruminants and Rift Valley fever in Saudi Arabia. PLoS One 10 (10): e0140328. https://doi.org/10.1371/journal.pone.0140328

Diniz AF, Santos B, Nobrega L, Santos VRL, Mariz WS, Cruz PSC, Nobrega RO, Silva RL, Paula AFR and Santos J, 2023. Antibacterial activity of *Thymus vulgaris* (thyme) essential oil against strains of Pseudomonas aeruginosa, Klebsiella pneumoniae and Staphylococcus saprophyticus isolated from meat product. Brazilian Journal of Biology 83: e275306. https://doi.org/10.1590/1519-6984.275306

Dursun N, Liman N, Özyazgan İ, Güneş I and Saraymen R, 2003. Role of thymus oil in burn wound healing. The Journal of Burn Care and Rehabilitation 24(6): 395-399. https://doi.org/10.1097/01.bcr.0000095513.67541.0f

Ejaz U, Afzal M, Mazhar M, Riaz M, Ahmed N, Rizg WY, Alahmadi AA, Badr MY, Mushtaq RY and Yean CY, 2024. Characterization, synthesis, and biological activities of silver nanoparticles produced via green synthesis method using *Thymus vulgaris* aqueous extract. International Journal of Nanomedicine 19: 453-469. https://doi.org/10.2147/ijn.s446017

Elbahnasawy AS, Valeeva E, El-Sayed EM and Rakhimov I, 2019. The impact of thyme and rosemary on prevention of osteoporosis in rats. Journal of Nutrition and Metabolism 2019, 1431384. https://doi.org/10.1155/2019/1431384

El-Readi MZ, Abdulkarim MA, Abdellatif AAH, Elzubeir ME, Refaat B, Althubiti M, Almaimani RA, Mukhtar MH, Al-Moraya IS and Eid SY, 2024. Doxorubicin-sanguinarine nanoparticles: formulation and evaluation of breast cancer cell apoptosis and cell cycle. Drug Development and Industrial Pharmacy 5:1-15. https://doi.org/10.1080/03639045.2024.2302557

Farooq AA, Khan MA, Akbar HA, Hayat MA, Murtaza SM, Shah MH, Javid MA, Saleem MU, Abdul Basit MA and Inayat SI, 2023. Effects of autologous bone marrow on the healing of long bones fractures reduced by external skeletal fixators in goats. Iraqi Journal of Veterinary Sciences 37: 963-9. https://doi.org/10.33899/IJVS.2023.137990.2759

Hajimehdipoor H, Shekarchi M, Khanavi M, Adib N and Amri M, 2010. A validated high performance liquid chromatography method for the analysis of thymol and carvacrol in *Thymus vulgaris* L. volatile oil. Pharmacognosy Magazine 6(23):154-8. https://doi.org/10.4103/0973-1296.66927

Heidari, Z, Salehzadeh, A, Sadat Shandiz SA and Tajdoost S, 2018. Anti-cancer and anti-oxidant properties of ethanolic leaf extract of *Thymus vulgaris* and its bio-functionalized silver nanoparticles. 3 Biotech 8(3):1778

Huo MH, Troiano NW, Pelker RR, Gundberg CM and Friedlaender GE, 1991. The influence of ibuprofen on fracture repair: biomechanical, biochemical, histologic, and histomorphometric parameters in rats. Journal of Orthopaedic Research 9(3): 383-90. https://doi.org/10.1002/jor.1100090310

Jahangirbasha D, Shivaprakash B, Dilipkumar D, Usturge S, Patil N, Tikare V and Bhagwantappa B, 2019. Retrospective Study on Incidence of Long Bone Fractures in Goats. Frontier Journal of Veterinary and Animal Sciences 8(1): (January-June). http://dx.doi.org/10.13140/RG.2.2.15136.80642

Kofler J, Hochschwarzer D, Schieder K, Osová A and Vidoni B, 2017. Limb fractures in 32 small ruminants-treatment and outcome. Tierarztl Prax Ausg G Grosstiere Nutztiere 45(4):201-21. https://doi.org/10.15653/tpg-160933

Leow JM, Clement ND, Tawonsawatruk T, Simpson CJ and Simpson AH, 2016. The radiographic union scale in tibial (RUST) fractures: Reliability of the outcome measure at an independent centre. Bone Joint Research 5 (4):116-21. https://doi:10.1302/2046-3758.54.2000628

Lozier JW, Niehaus AJ, Muir A and Lakritz J, 2018. Short-and long-term success of transfixation pin casts used to stabilize long bone fractures in ruminants. The Canadian Veterinary Journal 59(6):635–641. https://pmc.ncbi.nlm.nih.gov/articles/PMC5949959/

Maleki H, Doostan M, Khoshnevisan K, Baharifar H, Maleki SA and Fatahi MA, 2024. Zingiber officinale and *Thymus vulgaris* extracts co-loaded polyvinyl alcohol and chitosan electrospun nanofibers for tackling infection and wound healing promotion. Heliyon 10(1):e23719. https://doi.org/10.1016/j.heliyon.2023.e23719

Marsich E, Bellomo F, Turco G, Travan A, Donati I and Paoletti S, 2013. Nano-composite scaffolds for bone tissue engineering containing silver nanoparticles: preparation, characterization and biological properties. Journal of Materials Science: Materials in Medicine 24(7):1799-807. https://doi.org/10.1007/s10856-013-4923-4

Mohammadi M, Shahisaraee SA, Tavajjohi A, Pournoori N, Muhammadnejad S, Mohammadi SR, Poursalehi R and Delavari HH, 2019. Green synthesis of silver nanoparticles using Zingiber officinale and *Thymus vulgaris* extracts: characterisation, cell cytotoxicity, and its antifungal activity against Candida albicans in comparison to fluconazole. IET

Nanobiotechnology 13(2): 114-119. https://doi.org/10.1049/iet-nbt.2018.5146

Mollarafie, P, Khadiv Parsi P, Zarghami R, Amini FM and Ghafarzadegan R, 2015. Antibacterial and wound healing properties of thymol (*Thymus vulgaris* Oil) and its application in a novel wound dressing. Journal of Medicinal Plants 14: 69-81. http://jmp.ir/files/site1/user_files_8d9738/rezaghafary-A-10-218-3-fc7525e.pdf

Panah KG, Hesarak S and Farahpour MR, 2014. Histopathological evaluation of *Thymus vulgaris* on wound healing. Indian Journal of Fundamental and Applied Life Sciences 4 (S4): 3538-3544. http://www.cibtech.org/sp.ed/jls/2014/04/jls.htm

Pandiyan I, Sri SD, Indiran MA, Rathinavelu PK, Prabakar J and Rajeshkumar S, 2022. Antioxidant, anti-inflammatory activity of *Thymus vulgaris*-mediated selenium nanoparticles: An: in vitro: study. Journal of Conservative Dentistry and Endodontics 25(3): 241-245. https://doi.org/10.4103/jcd.jcd_369_21

Qing T, Mahmood M, Zheng Y, Biris AS, Shi L and Casciano DA, 2018. A genomic characterization of the influence of silver nanoparticles on bone differentiation in MC3T3-E1 cells. Journal of Applied Toxicology 38(2): 172-179. https://doi.org/10.1002/jat.3528

Ranoszek-Soliwoda K, Tomaszewska E, Socha E, Krzyczmonik P, Ignaczak A, Orlowski P, Krzyzowska M, Celichowski G and Grobelny J, 2017. The role of tannic acid and sodium citrate in the synthesis of silver nanoparticles. Journal of Nanoparticle Research 19(8): 273. https://doi.org/10.1007/s11051-017-3973-9

Sadan M, Naem M, Tawfeek HM, Khodier MM, Zeitoun MM, El-Khodery S, Alkhamiss AS, Hassan YAH and Abdellatif AAH, 2024. Can silver nanoparticles stabilized by Fenugreek (*Trigonella foenm -graecum*) improve tibial bone defects repair in rabbits? A preliminary study. Open Veterinary Journal 14(5): 1281-1293. https://doi.org/10.5455/ovj.2024.v14.i5.23

Sadan M, Almundarij R, Haridy M, EL-Khodery S, Elzarei MF, Abo-Aziza FAM, Ibrahim Z and Abdellatif AAH, 2025. Can Silver Nanoparticles Stabilized by Shilajit (Asphaltum punjabianum) accelerate Tibial Bone Defects Repair in Rabbits: A Preliminary Study. International Journal of Veterinary Science 14(3): 512-519. https://doi.org/10.47278/journal.ijvs/2024.276

Sakhaee E, Samimi AS and Mashayekhi S, 2024. Prediction of postpartum subclinical hypocalcemia using prepartum serum macromineral concentrations in Saanen and Beetal dairy goats. Comparative Clinical Pathology 33: 69-74. https://doi.org/10.1007/s00580-023-03523-9

Selmi S, Alimi D, Rtibi K, Jedidi S, Grami D, Marzouki L, Hosni K and Sebai H, 2022. Gastroprotective and Antioxidant Properties of Trigonella foenum graecum Seeds Aqueous Extract (*Fenugreek*) and Omeprazole Against Ethanol-Induced Peptic Ulcer. Journal of Medicinal Food 25(5): 513-522. https://doi.org/10.1089/jmf.2020.0217

Sindhu R, Reddy PVV and Saran S, 2024. Incidence of Long Bone Fractures in Goat and Sheep–A Study Report. The Indian Veterinary Journal 101(1): 28-30. https://doi.org/10.62757/IVA.2024.101.1.28-30

Sravanti M, Chandra Sekhar E, Latha C, Pramod Kumar D and Lakshman M, 2022. Haemato-biochemical changes of external skeletal fixation on long bone fractures in sheep and goats. The Pharma Innovation Journal 11(4S): 1315-1319

Steinigeweg D and Schlucker S, 2012. Monodispersity and size control in the synthesis of 20-100 nm quasi-spherical silver nanoparticles by citrate and ascorbic acid reduction in glycerol-water mixtures. Chemical Communications 48(69): 8682-8684. https://doi.org/10.1039/c2cc33850e

Taha SM, Abd El-Aziz NK, Abdelkhalek A, Pet I, Ahmadi M and El-Nabtity SM, 2024. Chitosan-Loaded Lagenaria siceraria and *Thymus vulgaris* Potentiate Antibacterial, Antioxidant, and Immunomodulatory Activities against Extensive Drug-Resistant Pseudomonas aeruginosa and Vancomycin-Resistant Staphylococcus aureus: In Vitro and in Vivo Approaches. Antioxidants (Basel) 13(4): 428. https://doi.org/10.3390/antiox13040428

Tawfeek HM, Abdellatif AAH, Abdel-Aleem JA, Hassan YA and Fathalla D, 2020. Transfersomal gel nanocarriers for enhancement the permeation of lornoxicam. Journal of Drug Delivery Science and Technology 56: 101540. https://doi.org/10.1016/j.jddst.2020.101540

Tharwat M, 2020. Serum concentration of bone metabolism biomarkers in goats during the transition period. Veterinary Medicine International 2020: 4064209. https://doi.org/10.1155/2020/4064209

Varghese R, Almalki MA, Ilavenil S, Rebecca J and Choi KC, 2019. Silver nanopaticles synthesized using the seed extract of Trigonella foenum-graecum L. and their antimicrobial mechanism and anticancer properties. Saudi Journal of Biological Sciences 26(1): 148-154. https://doi.org/10.1016/j.sjbs.2017.07.001

Vijayaram S, Razafindralambo H, Sun Y-Z, Vasantharaj S, Ghafarifarsani H, Hoseinifar SH and Raeeszadeh M, 2024. Applications of green synthesized metal nanoparticles—a review. Biological Trace Element Research 202(1): 360-386. https://doi.org/10.1007/s12011-023-03645-9

Vimalraj S, 2020. Alkaline phosphatase: Structure, expression and its function in bone mineralization. Gene 754: 144855. https://doi.org/10.1016/j.gene.2020.144855

Xu L, Wang YY, Huang J, Chen CY, Wang ZX and Xie H, 2020. Silver nanoparticles: Synthesis, medical applications and biosafety. Theranostics 10 8996-9031. Xu L, Wang YY, Huang J, Chen CY, Wang ZX and Xie H, 2020. Silver nanoparticles: Synthesis, medical applications and biosafety. Theranostics 10(20): 8996-9031. https://doi.org/10.7150/thno.45413

Zillinger LS, Hustedt K, Schnepel N, Hirche F, Schmicke M, Stangl GI and Muscher-Banse AS, 2024. Effects of dietary nitrogen and/or phosphorus reduction on mineral homeostasis and regulatory mechanisms in young goats. Frontiers in Veterinary Science 11: 1375329. https://doi.org/10.3389/fvets.2024.1375329

In Press